ACS Medicinal Chemistry Letters

Letter

pubs.acs.org/acsmedchemlett

Synthesis and Biological Evaluation of New Quinoxaline Derivatives of ICF01012 as Melanoma-Targeting Probes

Radhia El Aissi,[†,‡] Jianrong Liu,[†,‡] Sophie Besse,[†,‡] Damien Canitrot,[†,‡] Olivier Chavignon,[†,‡] Jean-Michel Chezal,[†,‡] Elisabeth Miot-Noirault,[†,‡] and Emmanuel Moreau*[,†,‡]

[†]INSERM−Université d'Auvergne, UMR 990, IMTV, BP 184, F-63005 Clermont-Ferrand Cedex, France

[‡]Clermont Université, Université d'Auvergne, Imagerie Moléculaire et Thérapie Vectorisée, BP 10448, F-63005 Clermont-Ferrand Cedex, France

Supporting Information

ABSTRACT: The aim of this study was the synthesis and pharmacokinetic selection of a best melanin-targeting ligand for addressing anticancer agents to pigmented melanoma. Seven quinoxaline carboxamide derivatives were synthesized and radiolabeled with iodine-125. Biodistribution studies of compounds [^{125}I]**1a**−**g** performed in melanoma-bearing mice tumor showed significant tumor uptake (range 2.43−5.68%ID/g) within 1 h after i.v. injection. Fast clearance of the radioactivity from the nontarget organs mainly via the urinary system gave high tumor-to-blood and tumor-to-muscle ratios. Given its favorable clearance and high tumor-melanoma uptake at 72 h, amide **1d** was the most promising melanoma-targeting ligand in this series. Compound **1d** will be used as building block for the design of new melanoma-selective drug delivery systems.

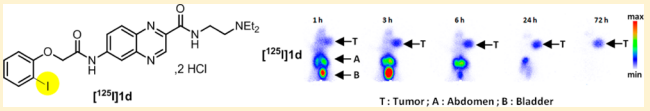

KEYWORDS: *Melanoma, melanin-targeting ligand, radiolabeling, iodine-125*

Disseminated melanoma is an incurable disease. Its prognosis has remained unchanged over the past 20 years. To date no treatment strategy has proved better than dacarbazine monochemotherapy, which remains the first line of treatment for this lethal form of skin cancer. Newly developed multidrug chemotherapy, biochemotherapy, and targeted therapy have all yielded disappointing results, with poorer quality of life and no real survival benefit for the patient.[1] However, the concept of targeted cancer therapy, which has emerged during the past decade, opens a wider therapeutic window than traditional cytotoxic drugs. An emblematic example is imatinib (STI571, Gleevec, Glivec), the first drug approved by the FDA that revolutionized the small molecular kinase inhibitor concept.[2] These targeted therapies improve anticancer treatment efficacy through interference with specific cellular pathways involved in tumor growth and progression. To increase antitumor efficacy while reducing systemic side effects, nanoparticles were used to permit an accumulation in certain solid tumors by EPR effect. For example, an albumin bound paclitaxel nanoparticle Abraxane was recently approved by the FDA for the treatment of breast cancer (2005) and for nonsmall cell lung cancer (2012).[3]

The key step in the development of an effective cancer treatment is based on the identification of the biological characteristics and/or pathways of individual tumors.[4] Regarding melanoma cancer, several mutations have been used to develop specific treatments (CDKN2A, CDK9, NSRAS, and BRAF).[5] Other targets have also been identified and investigated, such as sigma-1 and melanocortin-1 receptors and melanin pigments.[6−9]

Since the 1990s our research group has focused on the development of radiotracers able to specifically bind to melanins for the diagnosis of disseminated melanoma. Several structure−activity relationship studies have demonstrated that the chemical scaffold of these compounds should contain an aromatic moiety together with a tertiary amino group to allow sufficient binding to melanins via ionic and π stacking interactions (Figure 1A).[8] Recently (2008−2013) a phase 3 clinical trial (compound **I**, called [^{123}I]BZA2) was initiated to evaluate the sensitivity and specificity of [^{123}I]BZA2 versus [^{18}F]FDG for the imaging of patients with melanoma.[10]

With the aim of increasing uptake and tumor retention for targeted radionuclide therapy application with iodine-131,

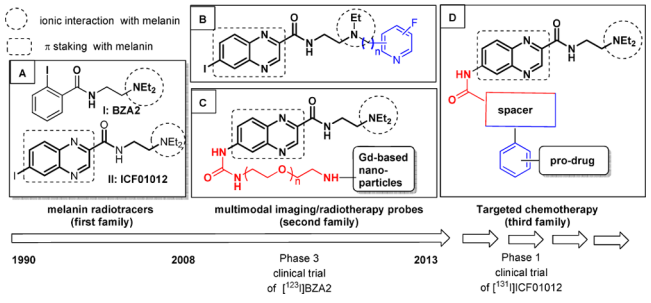

Figure 1. From clinical molecular imaging to preclinical targeted therapy of melanoma.

Received: November 15, 2013
Accepted: February 20, 2014
Published: February 20, 2014

optimization of the (hetero)aromatic moiety of BZA2 was designed.[11] The synthesized compounds were then tested in vivo to evaluate their biodistribution in the melanoma-bearing mouse model. Among all these new derivatives, quinoxaline radiotracer **II** (called [^{125}I]ICF01012) (Figure 1A) demonstrated a very favorable tumor uptake and dosimetry parameters.[11,12] Given its favorable pharmacological properties, it will be evaluated for clinical application in radionuclide therapy for disseminated melanoma ([^{131}I]ICF01012 (**II**)).[13] On the basis of our lead melanin-targeting ligand ICF01012, bimodal agents were developed and showed specific affinity for melanoma, allowing both early SPECT (^{123}I) or PET (^{18}F) imaging and efficient targeted radionuclide therapy (^{131}I) of melanoma.[14−16,18] These original radiotracers were synthesized by substituting one of the ethyl residues by an *N*-ethoxyfluoropyrinyl moiety (Figure 1B, blue part). The ICF01012 scaffold has also been conjugated to Gd-based nanoparticles for radiosensitizing purposes via the functionalization of the aromatic part (Figure 1C, red part). Biacore studies have shown that such modified particles bind efficiently to melanin pigments.[19]

Various strategies to treat melanoma based on melanin-targeted chemotherapy have also been studied in our laboratory. Despite very promising biodistribution profiles of acridine analogues of BZA or ICF01012 with DNA-intercalating properties,[20−22] only moderately good results have been obtained in melanoma mouse models. These disappointing results may be explained by the scavenger effect suggested by Chen et al., involving melanosomal sequestration of melanin-targeted chemotherapy.[23] On the basis of these findings, we decided to change our approach to a two-step prodrug targeted delivery strategy. First, the prodrug was to be addressed to the tumoral melanosomes using a melanin-targeting ligand. The anticancer agent would then be released by tumor selective cleavage.

To investigate this concept of melanoma-directed prodrug therapy, we examined a novel family of melanin-targeting ligands combining an alkyl spacer and an aromatic platform based on ICF01012 (Figure 1D, blue and red parts). We first designed and synthesized two subfamilies of ICF01012 analogues substituted by a 2-(iodoaryl)urea (or amide) alkyl chain at the C-6 position of the quinoxaline core. For compounds **1a−c**, we included a thioalkyl chain (Scheme 1a: X = S, m = 1) or an alkoxy chain in the chemical scaffold (Scheme 1b,c: X = O, m = 1, 4, respectively).

When the quinoxaline moiety was substituted by an amido group, with the length of alkyl chain ranging from one to five carbons (Figure 1, compounds **1d−g** with n = 1, 3, 4, or 5). Compounds **1a−g** were then radiolabeled with iodine-125 and evaluated in a melanoma-bearing mouse model to identify the best candidate presenting optimal melanin targeting properties and pharmacokinetic profile to help build a promising melanin-targeting pro-drug.

Scheme 1

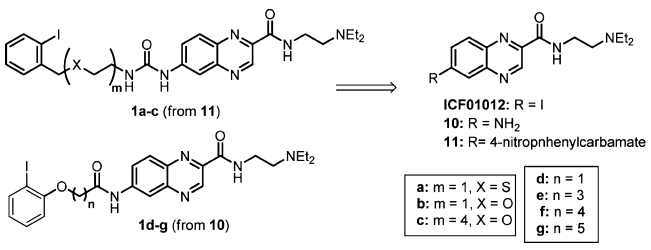

Results and Discussion. Access to compounds **1a−g** was achieved from the aminoquinoxaline derivative **10**[18] (for **1d−g**) and its corresponding carbamate **11**[18] (for **1a−c**) as starting materials with 2-(iodoaryl)amino derivatives **3a−c** or ω-(2-iodophenoxy)alkoxy acid derivative **3d−g**, respectively. Briefly, compounds **3a−c** were synthesized from 1-(bromomethyl)-2-iodobenzene **2**: a direct reaction with 2-mercaptoethamine yielded **3a**. Compound **3b** was obtained by nucleophilic substitution of **2** in the presence of *N*-Boc ethanolamine, followed by a deprotection under trifluoroacetic acid conditions. Compound **3c** was prepared in three steps. After monobenzylation of tetraethyleneglycol with 2-iodobenzyl bromide **2**, the terminal hydroxyl group of compound **5** was converted into iodo derivative **6**, which gave **3c** after a Gabriel reaction (Scheme 2).

Scheme 2[a]

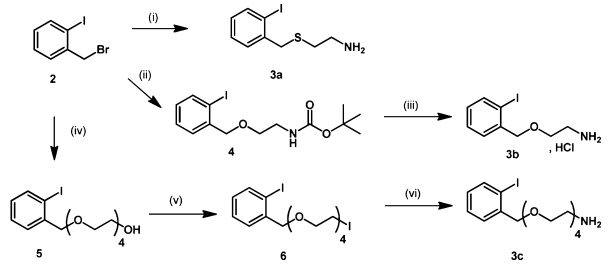

[a]Reactants and conditions: (i) 2-aminothioethanol hydrochloride, LiOH monohydrale, H_2O/EtOH (1/3, v/v), 35 °C; (ii) *tert*-butyl (2-hydroxyelhyl)coarbamate, KOH, dry dichloromelhane, rt; (iii) TFA, dry dichloromethane, rt; (iv) NaH, dry THF, rt; (v) imidazole, PPh_3, I_2, dry dichlorom ethane, rt; (vi) (a) potassium phtalimide, dry DMF, 30 °C; (b) hydrazine monohydrate, ethanol, 30 °C.

For compounds **3d−g**, after a first esterification of commercially available ω-halogenated acids (**7d−g**, n = 1, 3−5), an *O*-alkylation in anhydrous DMF in the presence of anhydrous potassium carbonate and 2-iodophenol was performed to give ethyl ω-(2-iodophenoxy)carboxylate compounds. Then, compounds **9d−g** were saponified with lithium hydroxide monohydrate and converted into acid **3d−g** after acidification (Scheme 3).

Scheme 3[a]

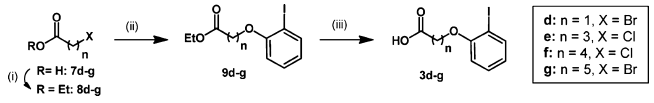

[a]Reactants and conditions: (i) acetyl chloride, dry ethanol, rt; (ii) 2-iodophenol, dry DMF, 80 °C; (iii) (a) LiOH monohydrate, THF/H_2O/MeOH (3/1/1, v/v/v), rt; (b) HCl (1 N).

Finally, compounds **1a−g** were synthesized as outlined in Scheme 4. Urea derivatives **1a−c** were obtained from **11** and DMAP with the appropriate amino derivatives **3a−c** in moderate yields (44−66%). Access to amido derivatives **1d−g** was achieved from derivatives **3d−g**: after treatment of these acids with thionyl chloride, adding amine **10** afforded **1d−g** with yields in the range 29−98%.

For a whole-body distribution study, seven quinoxaline derivatives (**1a−g**) were radioiodinated at low specific activity

dx.doi.org/10.1021/ml400468x | ACS Med. Chem. Lett. 2014, 5, 468−473

Scheme 4[a]

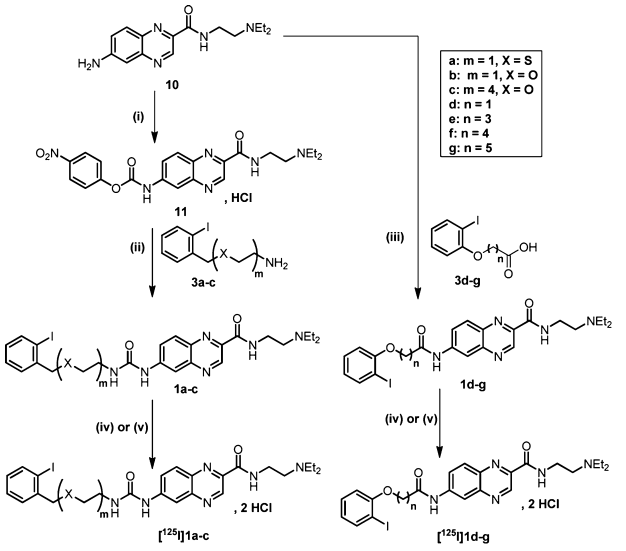

[a]Reagents and conditions: (i)4-nitrophenylchloroformate, pyridine, dry DCM, rt; (ii) **3a–c**, DMAP, dryTHF, TA; (iii) (a) **3d–g**, thionyl chloride, dry DCM, 45 °C; b) 10, DMAP, dry DCM, 45 °C; (iv) 2 N HCl diethyl ether, rt; (v) (a) $Na^{125}I$, acetic acid, 130 °C; (b) 2 N HCl diethyl ether, rt.

using a nucleophilic aromatic isotopic exchange reaction with no-carrier-added [^{125}I]NaI in the presence of $CuSO_4$ at 130 °C.[8] For each radiotracer, the following radiolabeling reaction parameters were optimized: reaction time (15–45 min) and acid conditions (method A, acetic acid; method B, citrate buffer) (Table S1, Supporting Information).

After purification by semipreparative radio-reversed phase-high pressure liquid chromatography analyses, compounds [^{125}I]**1a–g** were converted to hydrochloride salts (more soluble in aqueous medium) with good radiochemical yields (RCY, 43–56%), high radiochemical purities (RCP > 98%), and with a specific activity (SA) in the range 18.5–37.3 MBq/μmol. Reaction conditions and radiochemical data are reported in the Supporting Information (Tables S1–S3). All the radiotracers studied showed a very high chemical stability when incubated in physiological serum (NaCl 0.9%) at 37 °C for 24 h (RCP > 97%).

In ongoing work to design quinoxaline derivatives for tumor-targeted melanoma chemotherapy, the first challenge was to maintain a high affinity for melanin. Compared with the standard ICF01012, all the newly synthesized quinoxaline derivatives [^{125}I]**1a–g** displayed a strong affinity for synthetic melanin in water (Table 1).

Similarly to the previous results obtained with [^{125}I]-**ICF01012**, the binding of [^{125}I]**1** to synthetic melanin in PBS significantly decreased except for urea [^{125}I]**1a**. However, molecular binding to synthetic melanin was better than that observed with BZA or similar to ICF01012 data.[11] The lipophilicity values (log *P* (*n*-octanol/PBS), Table 1) of the compounds studied were all higher than those obtained for ICF01012 (range 1.25–2.07 for log *P* (**1a–g**) vs. 1.12 for log *P* (ICF01012)). The lipophilic character of the compounds studied seemed to some extent be related to melanin binding affinity in PBS except for [^{125}I]**1f**. Nevertheless, for compounds [^{125}I]**1a–g**, it was difficult to establish a correlation between melanin binding affinity and log *P* values. Analysis of the data obtained in these experiments showed that melanin binding

Table 1. In Vitro Binding to Melanin and log *P* of [^{125}I]1a–g

	% bound to synthetic melanin		
compd	H_2O	PBS	log P^a
[^{125}I]**1a**	92.8 ± 0.6	87.7 ± 0.6	2.06 ± 0.03
[^{125}I]**1b**	96.2 ± 0.7	74.0 ± 1.2	1.76 ± 0.04
[^{125}I]**1c**	94.0 ± 0.1	81.0 ± 0.4	1.89 ± 0.07
[^{125}I]**1d**	93.9 ± 0.4	73.3 ± 3.1	1.25 ± 0.03
[^{125}I]**1e**	96.0 ± 0.7	86.4 ± 2.5	2.07 ± 0.04
[^{125}I]**1f**	96.0 ± 0.2	86.5 ± 0.2	1.30 ± 0.05
[^{125}I]**1g**	95.0 ± 2.7	68.4 ± 4.2	1.33 ± 0.04
[^{125}I]**ICF01012**[b]	96.8 ± 0.5	72.1 ± 1.0	1.12

[a]Partition coefficient between *n*-octanol and phosphate buffer solution (PBS, pH 7.4). [b]For ICF01012, binding melanin and log *P* values were obtained from previous work.[3]

affinity increased with log *P* values for urea series (compounds [^{125}I]**1a–c**). For amide series, an interpretation of the data was complex: indeed, the affinity was similar (86%) for [^{125}I]**1f** and [^{125}I]**1e**, but log *P* values were very different (log *P* ([^{125}I]**1f**) = 1.30 vs log *P* ([^{125}I]**1e**) = 2.07). Moreover, log *P* values were similar for [^{125}I]1f and [^{125}I]**1g**, but the melanin affinity of [^{125}I]**1g** decreased dramatically. We concluded no correlation between lipophilicity and melanin binding in water and in PBS

Whole body distribution was assessed by scintigraphic imaging performed at 1, 3, 24, and 72 h post-i.v. injection (3.7 MBq/0.2 mL of NaCl 0.9%) (Figures S1 and S2, Supporting Information). Biodistribution in tumor and organs was evaluated by ex vivo counting at the same time-points. Intravenous administration of ^{125}I- radiolabeled compounds was well tolerated, with no evidence over 72 h of side effects such as lethargy, rough coat, and closed eyes. For [^{125}I]**1a–g**, high B16F0 melanoma uptakes were observed as early as 1 h postinjection (p.i.), ranging from 1.05 to 2.22 and 2.43 to 5.68%ID/g for urea and amido compounds, respectively (Table 2). We noted a similar radioactivity uptake profile in the pigmented structures of eyes. These results were consistent with a melanin binding uptake mechanism as previously described and observed by us[24] with different *N*,*N*-diethylethylenamino aryl compounds.[14–16] Considering the highly pigmented eyes of the C57BL6J model, these observations have to be interpreted carefully on the basis of the melanin content differences between humans and animal eyes, as recently published by Durairaj et al.[17]

For all the compounds evaluated, tumor retention was observed over 72 h (range 0.30–2.72%ID/g).

For the urea series, tumor accumulation of [^{125}I]**1a–c** was observed to be as early as 1 h after i.v. administration, with for [^{125}I]**1c** a high value of 2.22% ID/g peaking at 3 h p.i. (3.18% ID/g) and then decreasing rapidly to 0.71% ID/g at 24 h and 0.61% ID/g at 72 h. A similar profile was observed for [^{125}I]**1a b** (Table 2). For the three urea compounds, similar biodistribution profiles were also observed in eyes between 3 and 72 h. We noted a rapid release from nontarget tissues leading to rapidly unquantifiable ratios when organ concentration was within the range of the background value (Table S2, Supporting Information) for compound [^{125}I]**1a,c**. Only compound [^{125}I]**1b** showed sustained liver and kidney uptakes of 0.22 and 0.33%ID/g at 24 h p.i., respectively.

For the amide series, compounds [^{125}I]**1d–g** exhibited a tumor affinity three times higher than [^{125}I]**1a-c**, ranging from 2.43 to 5.68% ID/g at 1 h p.i. Similarly, from 24 h p.i., %ID/g values of [^{125}I]**1d–g** were higher than the maximum values

dx.doi.org/10.1021/ml400468x | ACS Med. Chem. Lett. 2014, 5, 468–473

Table 2. Biodistribution of [^{125}I]1a-g Compared with ICF01012 at Various Times after i.v. Administration in B16F0 Melanoma-Bearing Mice

compd	time (h)	melanoma[a]	eyes[a]	thyroid and SG[a,b]
[^{125}I]**1a**	1	1.05 ± 0.15	1.58 ± 0.07	3.87 ± 0.17
	3	1.15 ± 0.32	1.62 ± 0.18	3.18 ± 0.61
	24	0.83 ± 0.26	1.67 ± 0.38	1.54 ± 0.67
	72	0.37 ± 0.14	1.36 ± 0.56	0.99 ± 0.34
[^{125}I]**1b**	1	1.92 ± 1.02	2.21 ± 0.11	3.93 ± 1.24
	3	2.03 ± 0.09	3.22 ± 0.11	2.01 ± 0.01
	24	1.27 ± 0.70	2.50 ± 1.16	0.74 ± 0.21
	72	0.87 ± 0.50	2.91 ± 0.57	1.69 ± 1.19
[^{125}I]**1c**	1	2.22 ± 0.05	1.97 ± 0.41	1.99 ± 0.13
	3	3.18 ± 0.72	2.39 ± 0.59	1.35 ± 0.83
	24	0.71 ± 0.01	1.32 ± 0.09	0.66 ± 0.03
	72	0.61 ± 0.26	1.41 ± 0.28	1.37 ± 0.49
[^{125}I]**1d**	1	5.68 ± 1.16	5.67 ± 0.30	4.12 ± 0.86
	3	5.60 ± 1.56	6.46 ± 0.18	1.16 ± 0.20
	24	3.30 ± 0.75	4.88 ± 1.98	0.33 ± 0.04
	72	2.40 ± 0.30	7.04 ± 2.35	0.43 ± 0.12
[^{125}I]**1e**	1	2.43 ± 0.39	2.66 ± 0.83	2.19 ± 0.33
	3	1.86 ± 0.50	1.89 ± 0.64	0.49 ± 0.03
	24	1.67 ± 0.10	2.05 ± 0.15	0.72 ± 0.31
	72	0.75 ± 0.29	2.28 ± 0.61	0.73 ± 0.51
[^{125}I]**1f**	1	5.74[d]	4.96[d]	5.87[d]
	3	4.55 ± 1.15	4.40 ± 0.19	3.63 ± 0.05
	24	5.60 ± 2.10	6.93 ± 2.88	1.01 ± 0.07
	72	2.72 ± 1.76	7.15 ± 1.76	0.70 ± 0.20
[^{125}I]**1g**	1	3.62 ± 0.09	3.90 ± 0.16	6.08 ± 0.41
	3	5.82 ± 1.26	5.54 ± 0.27	3.75 ± 0.12
	24	2.99 ± 0.57	4.64 ± 0.91	0.89 ± 0.01
	72	2.64 ± 0.37	7.30 ± 0.42	1.14 ± 0.32
ICF01012[e]	1	17.0 ± 11.1	33.82 ± 3.47	*c*
	3	27.7 ± 7.0	24.79 ± 6.78	39.76 ± 23.47
	24	21.7 ± 10.8	32.30 ± 6.52	94.22 ± 27.48
	72	12.45 ± 1.6	25.26 ± 8.38	*c*

[a]Radioactive concentration values are expressed as means of %ID/g to ± SD (two mice, *n* determinations for each compound at each time point). [b]SG: submaxillary glands. [c]No value: no radioactive signal detected in the tissue. [d]No standard deviation when only one determination was made per organ. [e]ICF01012 values were obtained from previous work.[11]

observed from [^{125}I]**1a−c** over a period of 72 h (3.18−5.60% ID/g for [^{125}I]**1d−g** vs 1.15−3.18%ID/g for [^{125}I]**1a−c**). For [^{125}I]**1d−g**, we observed a melanoma uptake twice higher at 72 h than compounds [^{125}I]**1a−c** except for [^{125}I]**1e**. For amido quinoxaline derivatives, no measurable activity in liver, kidney, blood, muscle, thyroid, or SG tissues was detected after 24 h (Table S4, Supporting Information). Such profiles offer high tumor/nontarget ratios (Table 3) and a rapid clearance of the radioactivity from the nontarget organs (Table S3, Supporting Information). Considering melanoma uptake and tumor/muscle ratio, compound [^{125}I]**1d** appears to be the most promising ICF01012 derivatives among the seven new synthesized derivatives. Compared with [^{125}I]ICF01012, compound [^{125}I]**1d** exhibited a lower tumoral uptake, but a higher clearance over the 24−72 h period.

As illustrated in Figure 2, a high tumor to nontarget ratio could be evidenced from 3 h post injection. The scintigraphic imaging performed after i.v. injection of [^{125}I]**1d** is reported in Figure 3. The images illustrate the accumulation in the tumor as

Table 3. Melanoma/Organ Ratios of [^{125}I]1a−g and ICF01012 Uptake in B16 Melanoma-Bearing Mice at Different Times after Injection

compd	time (h)	T/L[a]	T/M[a]	T/B[a]	T/E[a]	T/TSG[a]
[^{125}I]**1a**	1	0.12	1.72	2.14	0.66	0.27
	3	0.66	3.59	6.05	0.71	0.36
	24				0.49	0.54
	72				0.27	0.37
[^{125}I]**1b**	1	0.30	2.66	3.31	0.87	0.49
	3	1.26	5.97	10.15	0.63	1.01
	24	5.77			0.51	1.72
	72	6.21			0.30	0.51
[^{125}I]**1c**	1	1.09	8.53	3.26	1.12	1.12
	3	2.81	24.46	6.49	1.33	2.36
	24				0.54	1.08
	72				0.43	0.45
[^{125}I]**1d**	1	0.91	6.60	3.40	1.00	1.38
	3	3.36	20.74	4.91	0.87	4.83
	24				0.67	10.00
	72				0.34	5.58
[^{125}I]**1e**	1	0.47	3.42	4.11	0.91	1.11
	3	2.24	15.5	9.3	0.98	3.79
	24				0.81	2.32
	72				0.33	1.03
[^{125}I]**1f**	1	0.36	3.73	4.99	1.16	0.98
	3	0.60	4.73	4.21	1.03	1.25
	24				0.81	5.54
	72				0.38	3.89
[^{125}I]**1g**	1	0.2	1.76	2.41	0.93	0.60
	3	0.84	6.33	8.82	1.05	1.55
	24	21.35			0.64	3.36
	72				0.36	2.32
ICF01012	1	1.29	8.33	4.92	0.50	
	3	3.12	32.20	9.51	1.11	0.69
	24	14.54	24.94	7.02	0.66	0.22
	72					

[a]L, liver; M, muscle; B, blood; E, eye; TSG, thyroid and submaxillary glands.

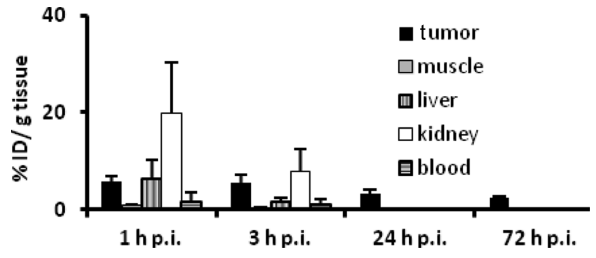

Figure 2. Radioactivity uptake in selected tissues after i.v. injection of [^{125}I]**1d** in B16F0 melanoma-bearing C57Bl/6J mice. Mean ± SD (two mice, *n* determinations at each time point).

early as 1 h post-i.v. injection, together with a rapid clearance from nontarget organs, mostly via the urinary excretion, allowing a well-defined contrast tumor from 6 h.

In this work we report the synthesis, radiolabeling with iodine-125, and biodistribution in B16F10 melanoma-bearing mice using scintigraphic imaging and organ counting of seven new quinoxaline derivatives. We demonstrate that the adjunction of a urea or amido phenyl group at the C-6 position of the ICF01012 scaffold did not modify the affinity for melanoma in vivo. On the basis of these results, we consider

dx.doi.org/10.1021/ml400468x | ACS Med. Chem. Lett. 2014, 5, 468−473

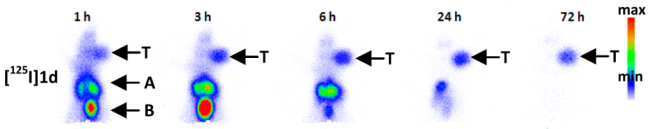

Figure 3. In vivo kinetics of compound [^{125}I]**1d** in a B16F0 melanoma-bearing C57Bl/6J mouse illustrated by serial planar scintigraphic images using a dedicated γ imager for small animals, at 1 h (A), 3 h (B), 6 h (C), 24 h (D), and 72 h (E) after a 37 MBq i.v. injection dose (acquisition time = 10 min). T, tumor; A, abdomen; B, bladder.

that compound **1d** presents the most favorable in vivo behavior for the future design of melanoma directed pro-drug delivery systems (Figure 1, third family). Consequently, chemical ligation of compound **1d** with a spacer that incorporates a predetermined breaking point allowing the drug to be released at the melanoma tumor site,[25,26] as previously evaluated by us,[27] is being investigated.

Experimental Section. *General Method for Synthesis of Quinoxaline Derivatives **1a–c**.* To a solution of 4-nitrophenyl (2-((2-(diethylamino)ethyl)carbomoyl)quinoxalin-6-yl)-carbamate (**11**) (1.1 equiv) dissolved in dry THF (20 mL), was added 1.65 equiv of DMAP, and the resulting mixture was stirred at room temperature for 30 min. The appropriate amine derivative (**3a–c**) (1 equiv) dissolved in dry THF (20 mL) was then added dropwise. The reaction mixture was stirred at room temperature until disappearance of the starting material as monitored by TLC. The reaction mixture was evaporated under reduced pressure. The crude product was dissolved with a saturated solution of $NaHCO_3$ (20 mL) and extracted with dichloromethane (3 × 40 mL). The pooled organic layers were washed with a saturated solution of $NaHCO_3$ (15 mL), water (15 mL), and brine (15 mL), dried over magnesium sulfate, filtered, and evaporated under reduce pressure.

*General Method for Synthesis of Quinoxaline Derivatives **1d–g**.* To a solution of the appropriate ω-(2-iodophenoxy)-alkoxy acid derivative (**3d–g**) (3.13 mmol, 6 equiv) dissolved in anhydrous DCM (20 mL) cooled to 0 °C, was added thionyl chloride (227 μL, 3.13 mmol, 6 equiv). The resulting mixture was refluxed for 5 h. After cooling to room temperature, excess solvent was coevaporated under reduced pressure with anhydrous toluene (3 × 10 mL). The residue was dissolved in anhydrous DCM (20 mL). 4-Dimethylaminopyridine (76.5 mg, 0.63 mmol, 1.2 equiv) and 6-amino-*N*-(2-(*N*,*N*-diethylamino)ethyl)quinoxaline-2-carboxamide (**10**) (0.15 g, 0.52 mmol, 1 equiv) were then added. The resulting mixture was heated at 45 °C for 18 h. After cooling to room temperature, a saturated solution of sodium carbonate (20 mL) was added. The aqueous solution was extracted with DCM (3 × 20 mL). The combined organic layers were dried over magnesium sulfate, filtered, and evaporated under reduced pressure.

■ ASSOCIATED CONTENT

Ⓢ Supporting Information

General methods for the synthesis of **1a–g**, **3a–g**, **4–6**, **8d–g**, **9d–g**, and **11**, radiolabeling of [^{125}I]**1a–g**. Full experimental details, ^{1}H and ^{13}C NMR, IR, and SM data for synthesized compounds **1a–g**, **3a–g**, **4–6**, **8d–g**, **9d–g**, and **11**. General methods for partition coefficient measurements, in vitro binding to melanin, cell culture, biodistribution in B16F0 melanoma bearing mice, scintigraphic imaging, and ex vivo biodistribution studies. Tables S1, S2, S3, and S4, Figures S1 and S2, and procedures for radiolabeling and biodistribution ratios. This material is available free of charge via the Internet at http://pubs.acs.org.

■ AUTHOR INFORMATION

Corresponding Author

*(E.M.) Phone: (33) 4 73 15 08 06. Fax: (33) 4 73 15 08 01. E-mail: emmanuel.moreau@udamail.fr.

Author Contributions

All the authors contributed to the drafting of the manuscript. All authors have given their approval to the final version of the manuscript.

Notes

The authors declare no competing financial interest.

■ ABBREVIATIONS

i.v., intravenous; p.i., postinjection; BZA, arylcarboxamide; [^{18}F]FDG, 2-deoxy-2-(^{18}F)fluoro-D-glucose; SPECT, single-photon emission computer tomography; PET, positron emission tomography

■ REFERENCES

(1) Finn, L.; Markovic, S. N.; Joseph, R. W. Therapy for metastatic melanoma: the past, present and future. *BMC Med.* **2012**, 10–23.

(2) Blair, B. G.; Bardelli, A.; Park, B. H. Somatic alterations as the basis for resistance to targeted therapies. *J. Pathol.* **2014**, *232* (2), 244–254.

(3) Ping, M.; Russel, J. M. Paclitaxel nano-delivery systems: a comprehensive review. *J. Nanomed. Nanotechnol.* **2013**, *4* (2), 1000164.

(4) Kim, M.-S. Future cancer therapy with molecularly targeted therapeutics: challenges and strategies. *Biomol. Ther.* **2011**, *19*, 371–389.

(5) Ji, Z.; Flaherty, K. T.; Tsao, H. Molecular therapeutic approaches to melanoma. *Mol. Aspects Med.* **2010**, *31*, 194–204.

(6) Waterhouse, R. N.; Chapman, J.; Izard, B.; Donald, A.; Belkin, K.; O'Brien, J. C.; Collier, T. L. Examination of four ^{123}I-labeled piperidine-based sigma-receptor ligands as potential melanoma imaging agents: initial studies in mouse tumor models. *Nucl. Med. Biol.* **1997**, *24*, 587–593.

(7) Cantorias, M. V.; Figueroa, S. D.; Quinn, T. P.; Lever, J. R.; Hoffman, T. J.; Watkinson, L. D.; Carmack, T. L.; Cutler, C. S. Development of high-specific.activity ^{68}Ga-labeled DOTA-rhenium-cyclized α-MSH peptide analog to target MC1 receptors overexpressed by melanoma tumors. *Nucl. Med. Biol.* **2009**, *36*, 505–513.

(8) Michelot, J. M.; Moreau, M. F. C.; Veyre, A. J.; Bonafous, J. F.; Bacin, F. J.; Madelmont, J. C.; Bussiere, F.; Souteyrand, P. A.; Mauclaire, L. P.; Chossat, F. M.; Papon, J. M.; Labarre, P. G.; Kauffmann, P.; Plagne, R. J. Phase II scintigraphic clinical trial of malignant melanoma and metastases with iodine-123-*N*-(2-diethylaminoethyl-4-iodobenzamide). *J. Nucl. Med.* **1993**, *34* (8), 1260–1266.

(9) Dadachova, E.; Moadel, T.; Schweitzer, A. D.; Bryan, R. A.; Zhang, T.; Mints, L.; Revskaya, E.; Huang, X.; Ortiz, G.; Nosanchuk, J. S.; Nosanchuk, J. D.; Casadevall, A. Radiolabeled melanin-binding peptides are safe and effective in treatment of human pigmented melanoma in a mouse model of disease. *Cancer Biother. Radiopharm.* **2006**, *21*, 117–129.

(10) Cachin, F.; Miot-Noirault, E.; Gillet, B.; Isnardi, V.; Labeille, B.; Payoux, P.; Meyer, N.; Cammilleri, S.; Gaudy, C.; Razzouk-Cadet, M.; Lacour, J. P.; Granel-Brocard, F.; Tychyj, C.; Benbouzid, F.; Grange, J.-D.; Baulieu, F.; Kelly, A.; Merlin, C.; Mestas, D.; Gachon, F.; Chezal, J.-M.; Degoul, F.; D'Incan, M. ^{123}I-BZA2 as a melanin-targeted radiotracer for the identification of melanoma metastases: results and perspectives of a multicenter phase III clinical trial. *J. Nucl. Med.* **2014**, *55* (1), 15–22.

(11) Chezal, J.-M.; Papon, J.; Labarre, P.; Lartigue, C.; Galmier, M.-J.; Decombat, C.; Chavignon, O.; Maublant, J.; Teulade, J.-C.; Madelmont, J.-C.; Moins, N. Evaluation of radiolabeled (hetero)-aromatic analogues of *N*-(2-diethylaminoethyl)-4-iodobenzamide for imaging and targeted radionuclide therapy of melanoma. *J. Med. Chem.* **2008**, *51* (11), 3133−3144.
(12) Chezal, J.-M.; Dollé, F.; Madelmont, J.-C.; Maisonial, A.; Miot-Noirault, E.; Moins, N.; Papon, J.; Kuhnast, B.; Tavitian, R.; Boisgard, R. World Patent WO 2009095872, 2009.
(13) Degoul, F.; Borel, M.; Jacquemot, N.; Besse, S.; Communal, Y.; Mishellany, F.; Papon, J.; Penault-Llorca, F.; Donnarieix, D.; Doly, M.; Maigne, L.; Miot-Noirault, E.; Cayre, A.; Cluzel, J.; Moins, N.; Chezal, J.-M.; Bonnet, M. In vivo efficacy of melanoma internal radionuclide therapy with a (131) I-labeled melanin-targeting heteroarylcarboxamide molecule. *Int. J. Cancer* **2013**, *133* (5), 1042−1053.
(14) Maisonial, A.; Kuhnast, B.; Papon, J.; Boisgard, R.; Bayle, M.; Vidal, A.; Auzeloux, P.; Rbah, L.; Bonnet-Duquennoy, M.; Miot-Noirault, E.; Galmier, M.-J.; Borel, M.; Askienazy, S.; Dollé, F.; Tavitian, B.; Madelmont, J.-C.; Moins, N.; Chezal, J.-M. Single photon emission computed tomography/positron emission tomography imaging and targeted radionuclide therapy of melanoma: new multimodal fluorinated and iodinated radiotracers. *J. Med. Chem.* **2011**, *54* (8), 2745−2766.
(15) Maisonial, A.; Billaud, E.-M.; Besse, S.; Rbah-Vidal, L.; Papon, J.; Audin, L.; Bayle, M.; Galmier, M.-J.; Tarrit, S.; Borel, M.; Askienazy, S.; Madelmont, J.-C.; Moins, N.; Auzeloux, P.; Miot-Noirault, E.; Chezal, J.-M. Synthesis, radioiodination and in vivo screening of novel potent iodinated and fluorinated radiotracers as melanoma imaging and therapeutic probes. *Eur. J. Med. Chem.* **2013**, *63*, 840−853.
(16) Billaud, E.-M.; Rbah-Vidal, L.; Vidal, A.; Besse, S.; Tarrit, S.; Askienazy, S.; Maisonial, A.; Moins, N.; Madelmont, J.-C.; Miot-Noirault, E.; Chezal, J.-M.; Auzeloux, P. Synthesis, radiofluorination and in vivo evaluation of novel fluorinated and iodinated radiotracers for PET imaging and targeted radionuclide therapy of melanoma. *J. Med. Chem.* **2013**, *56* (21), 8455−8467.
(17) Durairaja, C.; Chastainb, J. E.; Kompella, U. B. Intraocular distribution of melanin in human, monkey, rabbit, minipig and dog Eyes. *Exp. Eye Res.* **2012**, *98*, 23−27.
(18) Chezal, J.-M.; Rbah-Vidal L.; Billaud, E.; Auzeloux, P.; Madelmont, J.-C.; Vidal, A.; Miot-Noirault, E.; Papon, J.; Maisonial, A.; Moins, N. Labelled quinoxaline derivatives as multimodal radiopharmaceuticals and their precursors. WO 2013160808 A1.
(19) Morlieras, J.; Chezal, J.-M.; Miot-Noirault, E.; Roux, A.; Heinrich-Balard, L.; Cohen, R.; Tarrit, S.; Truillet, C.; Mignot, A.; Hachani, R.; Kryza, D.; Antoine, R.; Dugourd, P.; Perriat, P.; Janier, M.; Sancey, L.; Lux, F.; Tillement, O. Development of gadolinium based nanoparticles having an affinity towards melanin. *Nanoscale* **2013**, *5* (4), 1603−1615.
(20) Rapp, M.; Maurizis, J. C.; Papon, J.; Labarre, P.; Wu, T. D.; Croisy, A.; Guerquin-Kern, J. L.; Madelmont, J. C.; Mounetou, E. A new O6-alkylguanine-DNA alkyltransferase inhibitor associated with a nitrosourea (cystemustine) validates a strategy of melanoma-targeted therapy in murine B16 and human-resistant M4Beu melanoma xenograft models. *J. Pharmacol. Exp. Ther.* **2008**, *326* (1), 171−177.
(21) Desbois, N.; Gardette, M.; Papon, J.; Labarre, P.; Maisonial, A.; Auzeloux, P.; Lartigue, C.; Bouchon, B.; Debiton, E.; Blache, Y.; Chavignon, O.; Teulade, J.-C.; Maublant, J.; Madelmont, J.-C.; Moins, N.; Chezal, J. M. Design, synthesis and preliminary biological evaluation of acridine compounds as potential agents for a combined targeted chemo-radionuclide therapy approach to melanoma. *Bioorg. Med. Chem.* **2008**, *16* (16), 7671−7690.
(22) Gardette, M.; Papon, J.; Bonnet, M.; Desbois, N.; Labarre, P.; Wu, T. D.; Miot-Noirault, E.; Madelmont, J. C.; Guerquin-Kern, J. L.; Chezal, J. M.; Moins, N. Evaluation of new iodinated acridine derivatives for targeted radionuclide therapy of melanoma using ^{125}I, an Auger electron emitter. *Invest. New Drugs* **2011**, *29* (6), 1253−1263.
(23) Chen, K. G.; Valencia, J. C.; Lai, B.; Zhang, G.; Paterson, J. K.; Rouzaud, F.; Berens, W.; Wincovitch, S. M.; Garfield, S. H.; Leapman, R. D.; Hearing, V. J.; Gottesman, M. M. Melanosomal sequestration of cytotoxic drugs contributes to the intractability of malignant melanomas. *Proc. Natl. Acad. Sci. U.S.A.* **2006**, *123* (26), 9903−9907.
(24) Chehade, F.; De Labriolle-Vaylet, C.; Michelot, J.; Moins, N.; Moreau, M.-F.; Hindié, E.; Papon, J.; Escaig, F.; Galle, P.; Veyre, A. Distribution of I-BZA (*N*-2-diethylaminoethyl-4-iodobenzamide) in grafted melanoma and normal skin: a study by secondary ion mass spectroscopy. *Cell Mol. Biol.* **2001**, *47* (3), 529−534.
(25) Kratz, F.; Müller, I. A.; Ryppa, C.; Warnecke, A. Prodrug strategies in anticancer chemotherapy. *ChemMedChem* **2008**, *3* (1), 20−53.
(26) Singh, Y.; Palombo, M.; Sinko, P. J. Recent trends in targeted anticancer prodrug and conjugate design. *Curr. Med. Chem.* **2008**, *15* (18), 1802−1826.
(27) André, M.; Tarrit, S.; Couret, M.-J.; Galmier, M.-J.; Debiton, E.; Chezal, J.-M.; Mounetou, E. Spacer optimization of new conjugates for a melanoma-selective delivery approach. *Org. Biomol. Chem.* **2013**, *11* (37), 6372−6384.